CERN-ACC-NOTE-2018-0077

2016.11.29
Roberto.Rossi@cern.ch

Crystal Collimation Cleaning Measurements with Lead Ion Beams in LHC

R. Rossi, O. Aberle, O. O. Andreassen, M. Butcher, C. A. Dionisio Barreto, A. Masi, D. Mirarchi, S. Montesano, I. Lamas Garcia, S. Redaelli, W. Scandale, P. Serrano Galvez, A. Rijllart, G. Valentino, CERN, Geneva, Switzerland, F. Galluccio, INFN-Napoli, Naples, Italy

Keywords: LHC, collimation, crystal, UA9

Summary

During this MD, performed on November the 29th, 2016, bent silicon crystals were tested with lead ion beams for a possible usage of crystal-assisted collimation. Tests were performed both at injection energy and, for the first time, at flat top using both horizontal and vertical crystals. Loss maps at 6.5 TeV were measured to study the cleaning performances of crystal collimation with ion beam, and compared to that of the standard collimation system.

1 Introduction

During LS1, two bent crystals for beam collimation studies were installed in IR7, on beam 1. In 2015 the two crystals were tested, and channeling was successfully observed for both proton and ion beams, at injection and flat top[1] energy [1, 2, 5]. The cleaning efficiency of the standard LHC multi-stage collimation with ions is about 100 times worse than with protons. Crystal collimation could help to improve the ion cleaning. A first step towards the demonstration of feasibility of crystal collimation is the assessment of channeling of ion beam at the unprecedented beam energy of the LHC.

Tests in SPS comparing the performance of crystal system with protons and ions beam have already shown good results [6]. At the LHC, a setup has been conceived that uses only existing secondary collimators as absorbers for the channeled beam [7]. This layout is suitable for beam tests with proton and ion beams. The scope of this MD is to demonstrate that channeling can be achieved at top energy and that a good collimation cleaning can be produced with a reduced set - ideally with one - secondary collimator.

[1] Only for proton beams.

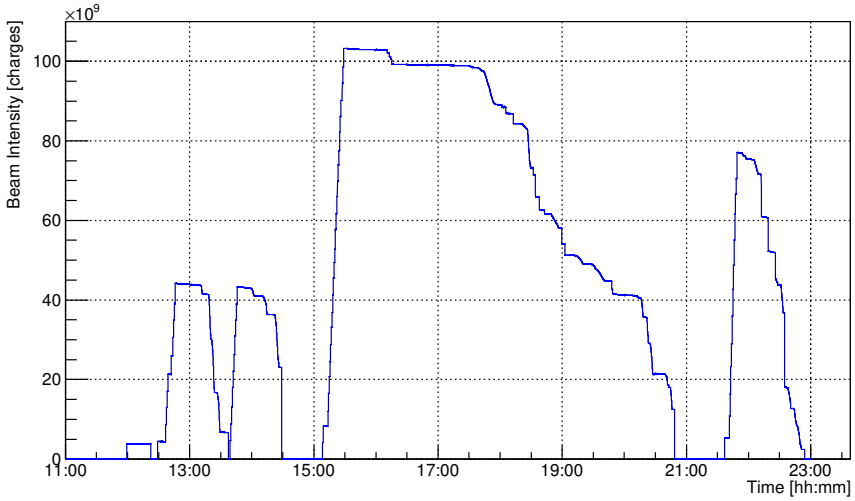

Figure 1: Beam availability during the MD.

In this note, the beam setup and machine configuration for the tests are presented. The results of beam measurements at injection and top energy are described in detail. Some initial conclusions are then drawn.

2 Beam Setup

The MD was performed using several low-intensity bunches at both injection and flat top energy with standard optics for ion beam on ring 1 (B1). The transverse dumper (ADT) was used to excite the beam with white noise, as in standard collimation loss maps, to achieve controlled primary beam losses on crystals and/or collimators. This was the reason why several low-intensity bunches have been accelerated to flat top energy. To have enough losses for the time needed to complete some measurements, such as angular scans [2], the ADT window was enlarged to act on three different bunches. This allows achieving for longer times sufficiently high loss rates. The overall LHC availability during those studies was good and is shown in Fig. 1 that shows the beam intensity as a function of time in the MD. All the scheduled measurements could be successfully performed.

The measurements involved the following main activities:

1) beam-based alignment of the crystal with respect to the beam orbit and transverse positioning as primary collimator;

2) angular scan for the determination of the channeling condition;

3) transverse scan of the channeled beam with a secondary collimator;

4) cleaning measurements through loss maps of a reduced collimation system based on a crystal in channeling position and different sets of secondary collimators.

The first step is performed in a similar way as a standard collimator jaw alignment and is not presented in detail. In the following section, the results of measurements (2), (3) are

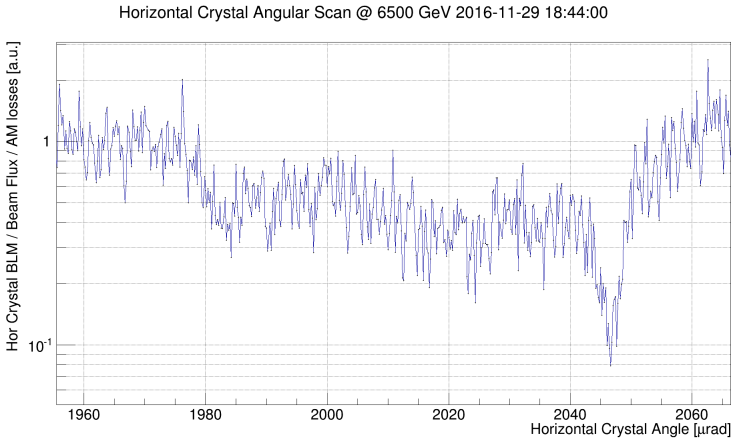

Figure 2: Horizontal crystal angular scan at top energy. Losses normalized to the beam flux as a function of the goniometer angle.

presented for both energies. Cleaning measurements (4) were performed for the first time with ion beams.

3 Measurements

3.1 Injection Energy Checks

The first operation of the MD was to repeat a minimal set of measurements for both horizontal and vertical crystals at injection energy, specifically the angular scans that allowed re-establishing the optimum channeling orientation angle. The detailed procedure described is well established from previous MDs, see for example [1]. Finding channeling at injection, when the beam can be efficiently injected, is a key asset for efficient measurements at top energy where all measurements must be carried out in a single fill. In previous MDs [2, 3, 5] the crystal bending angles was measured as 63.3 and 39.1 μrad for horizontal and vertical crystal, respectively.

3.2 Flat Top Energy Checks

The angular scans at flat top where performed with the settings listed in Tab. 1 (where operational settings are also given for reference). Onset of channeling is measurable as a reduction of the local beam losses, as in channeling the nuclear interactions with the crystals are suppressed compared to the losses through an amorphous material [8]. Once the optimum location is identified with a faster scan in the range identified during injection energy tests, slower scans are performed to measure in detail the whole range where coherent interactions (channeling, volume reflection [9]) between proton beam and crystal occur.

The results of the angular the "slow" angular scans of horizontal crystal is shown in Fig. 2. Three different bunches were used to complete the angular scan. Exiting one bunch while generating sufficiently high losses, would have consumed the bunch faster than the

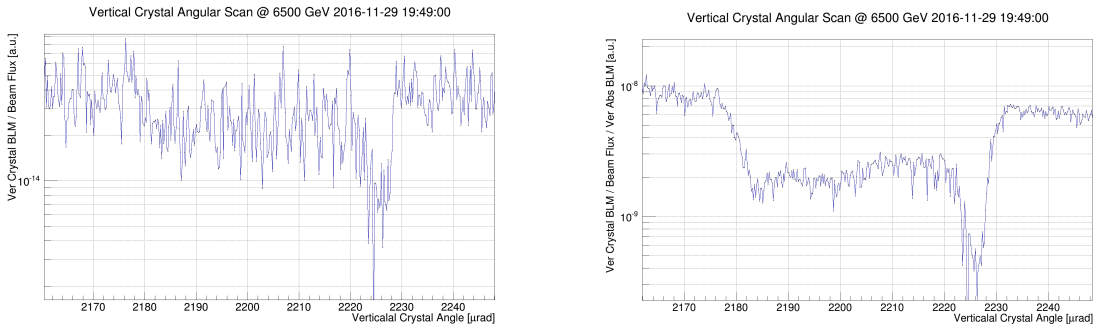

Figure 3: Vertical crystal angular scans at top energy. Losses normalized to the beam flux (Left) and to the absorber collimator local losses (Right), as a function of the goniometer angle.

time needed for an goniometer angular scan at the speed of 0.2 μrad/s used for precise measurements.

Losses recorded at 1 Hz, normalized to the bunch by bunch flux, and to the steady losses measurement with crystals in amorphous orientation, are used to produce the graph of Fig. 2. The beam flux is calculated fitting with a 3rd order polynomial function the slope in the beam current.

The vertical scan, instead, is affected by a lot of noise. Only by normalizing the crystal losses to the losses recorded at the monitor near the TCSG.D4L7 (first absorber for vertical crystal) it is possible to observe the standard crystal angular scan shape, as shown in Fig. 3 (Right). The two signals are correlated, but we cannot obtain informations, as the reduction factor of local losses is no longer measurable with such set of data.

Collimator IR7	Standard [σ]	Horizontal scan [σ]	Vertical scan [σ]
TCP	5.5	7.5	7.5
TCPCV	out	out	5.5
TCPCH	out	5.5	7.5
TCSG	7.5	7.5	7.5
TCLA	11.0	11.0	11.0

Table 1: IR7 Collimators positions (in σ units) during flat top standard operation and crystals scan operation.

3.3 Absorber Linear Scans

In order to characterize the properties of the channeled beam, a transverse scan with secondary collimators located downstream of the crystal was performed when it is oriented at its optimum angle for channeling. The secondary collimators TCSG.B4L7 and TCSG.D4L7 were used for horizontal and vertical crystal, respectively. During these measurements, all the collimators upstream of the secondary collimator used for the scan were opened. Inward and/or outward scans are performed by spanning the range in transverse amplitude between

the primary beam halo (closest position) and apertures where the collimator jaw does not intercept the channeled beam anymore. The measurement is given in Fig. 4, where the losses recorded downstream of the secondary collimator used for the scan are given as a function of the collimator jaw position. For the horizontal case (right plot) the bunches used were consumed before the completing the scan. This measurement was then dropped to use the remaining bunches for collimation cleaning measurements.

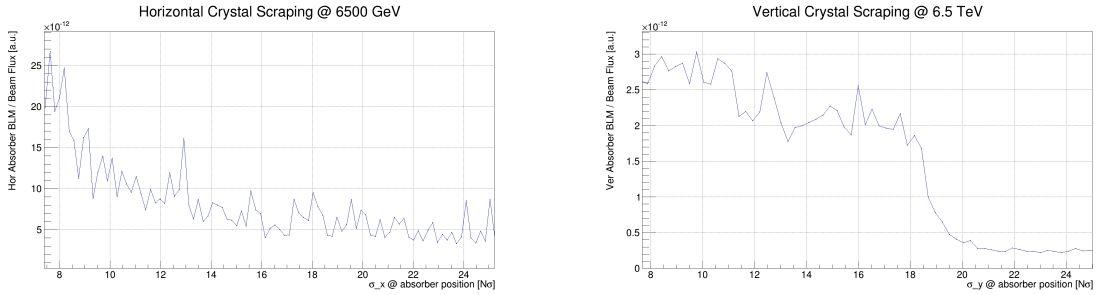

Figure 4: Horizontal (Left) and Vertical (Right) crystal channeled beam scrapings. Losses normalized to the beam intensity as a function of the absorber linear position.

Collimator	Standard [σ]	Horizontal [σ]					Vertical [σ]			
Configuration	Reference	1	2	3	4	5	1	2	3	4
TCP.D6L7	5.5	out	out	out	out	out	out	out	out	out
TCP.C6L7	5.5	out	out	out	out	out	out	out	out	out
TCP.B6L7	5.5	out	out	out	out	out	out	out	out	out
TCSG.A6L7	7.5	out	out	out	out	out	out	out	out	out
TCPCV.A6L7	out	out	out	out	out	out	5.5	5.5	5.5	5.5
TCSG.B5L7	7.5	out	out	out	out	out	out	out	out	out
TCSG.A5L7	7.5	out	out	out	out	out	out	out	out	out
TCSG.D4L7	7.5	out	out	out	out	out	7.5	7.5	7.0	8.0
TCPCH.A4L7	out	5.5	5.5	5.5	5.5	5.5	out	out	out	out
TCSG.B4L7	7.5	7.5	out	8.0	9.0	10.0	7.5	out	7.5	7.5
TCSG.A4L7	7.5	7.5	out	8.0	9.0	10.0	7.5	out	7.5	7.5
TCSG.A4R7	7.5	7.5	out	8.0	9.0	10.0	7.5	out	7.5	7.5
TCSG.B5R7	7.5	7.5	out	8.0	9.0	10.0	7.5	out	7.5	7.5
TCSG.D5R7	7.5	7.5	out	8.0	9.0	10.0	7.5	out	7.5	7.5
TCSG.E5R7	7.5	7.5	out	8.0	9.0	10.0	7.5	out	7.5	7.5
TCSG.6R7	7.5	7.5	7.5	8.0	9.0	10.0	7.5	out	7.5	7.5
TCLA.A6R7	11.0	11.0	11.0	11.0	11.0	11.0	11.0	11.0	11.0	11.0
TCLA.B6R7	11.0	11.0	11.0	11.0	11.0	11.0	11.0	11.0	11.0	11.0
TCLA.C6R7	11.0	11.0	11.0	11.0	11.0	11.0	11.0	11.0	11.0	11.0
TCLA.D6R7	11.0	11.0	11.0	11.0	11.0	11.0	11.0	11.0	11.0	11.0
TCLA.A7R7	11.0	11.0	11.0	11.0	11.0	11.0	11.0	11.0	11.0	11.0

Table 2: IR7 Collimators positions (in σ units) during flat top Loss Maps measurements.

4 Cleaning measurements

Loss maps were measured during this MD with both crystals at top energy. In standard collimation loss maps, the cleaning inefficiency is measured by normalizing all the monitors (BLM) to the losses recorded at primary collimator. This value is proportional to the number of halo particles intercepted by the collimation system, hence the losses in the dispersion suppressor region (DS) of IR7 give a direct measurement of collimation inefficiency. For crystal collimation, the highest losses occur at the collimator used as absorber so the same normalization would not produce comparable cleaning estimates.

Accurate flux measurements can evaluate the number of charges that are lost from the circulating beam and intercept the IR7 collimation system (standard or crystal-based). Hence, the normalization to the beam charge flux (calculated smoothing the beam intensity signals from fast BCT) is used to compare the two collimation system. The leakage factor is defined as the highest normalized loss value observed in IR7-DS during a loss map.

Standard collimation loss maps were measured as reference in the same fill. The variety of secondary collimators downstream the crystals allow comparing different kinds of setup to absorb the channeled halo particles. In Table 2 the different settings used are presented. The leakage ratios found in IR7-DS, on two different cold magnets position, and on momentum cleaning primary collimator (TCP IR3), are presented in Table 3, for all cases. For both planes, the case (1) indicate the present system with all TCSGs closes, and the case (2) indicate an ideal case where only one secondary collimator i used to intercept the channeled beam. Since the TCSG are made of 1m-long jaw of carbon, their absorption capability is limited and might not sufficient to absorb the channeled beam efficiently. This hypothesis must be assessed in simulations. In the MD, we explorer tighter TCSG setting scenarios as well. Note that, in order to optimize the cleaning performance, TCLA absorbers are all closes in all cases.

For the horizontal plane, we observed a slight improvement compared to the standard collimation. This is much below the expected performances of crystal collimation. It is also observable how reducing the set of TCSGs deteriorate the cleaning performances by a small factor. These aspect must be understood.

For vertical crystal, a comparable performance with respect to standard collimation is observed in IR7-DS. When a reduced set of TCSGs is used the system shows the same behavior observed for horizontal case. In fact, also in this case, a general deterioration of cleaning performances is measured.

5 Conclusions

The setup for crystal collimation tests in IR7 was tested, for the first time, at top energy with lead ion beam. For the first time, channeling was observed with both crystal, with lead ion beams at 6.5 Z TeV. This is a world record. Evidence of channeling comes from the monitoring of local losses downstream of the crystals, which are suppressed in channeling compared to amorphous orientations, and from scans of secondary collimators further downstream, which indicate the presence of a well-defined channeled halo separated from the beam core.

Plane	Configuration	Crystal Orientation	Leackage ratio Standard/Crystal	
			IR7-DS Q7	TCP IR3
H	1	CH	2.33	0.72
H	2	CH	1.87	0.55
H	3	CH	1.56	0.47
H	4	CH	2.00	0.62
H	5	CH	1.12	0.33
V	1	CH	1.07	0.89
V	2	CH	0.84	0.74
V	3	CH	0.76	0.63
V	4	CH	0.60	0.45

Table 3: IR7 Collimators positions (in σ units) during flat top standard operation and crystals scan operation.

Cleaning performances were tested for the first time for crystal collimation and directly compared to that of the present system. The crystal collimation did not reliably improve the cleaning performance. A deeper understanding of these data is needed and will be followed up in simulations.

6 Acknowledgements

The authors would like to thank the OP group for their assistance during the MD.

7 Appendix

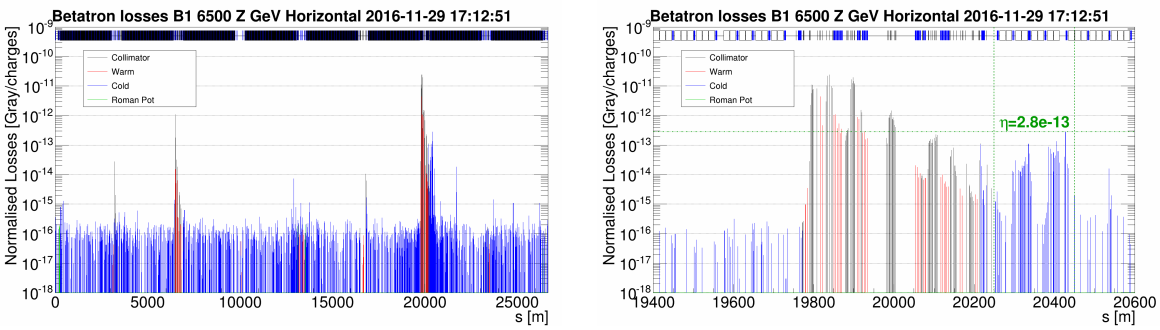

Figure 5: Horizontal standard loss maps. IR7 zoom is presented on the right.

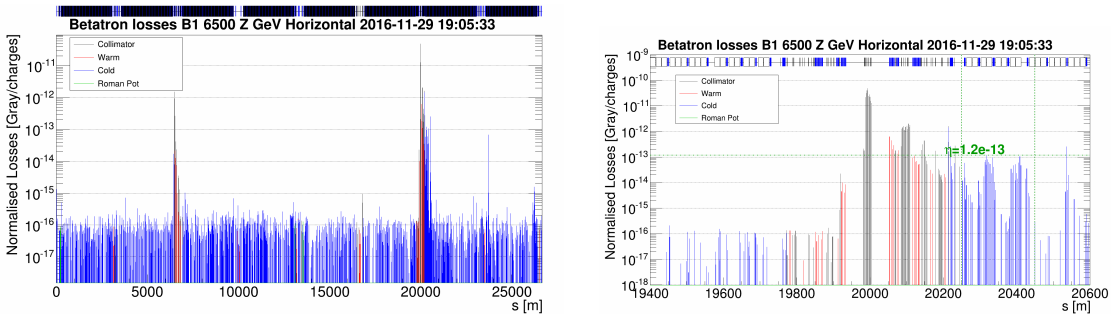

Figure 6: Horizontal crystal collimation loss maps. Settings 1 on Table 3. IR7 zoom is presented on the right.

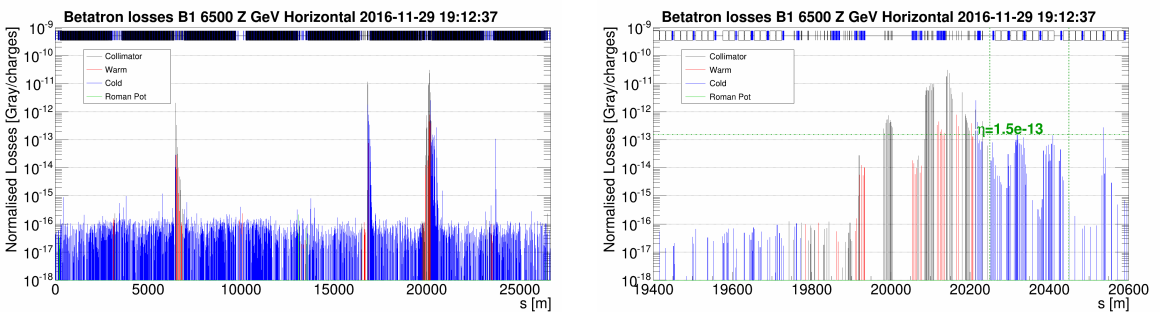

Figure 7: Horizontal crystal collimation loss maps. Settings 2 on Table 3. IR7 zoom is presented on the right.

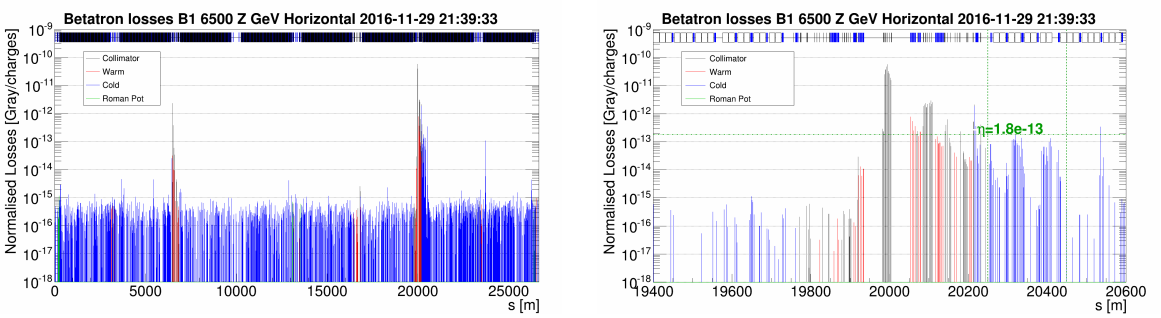

Figure 8: Horizontal crystal collimation loss maps. Settings 3 on Table 3. IR7 zoom is presented on the right.

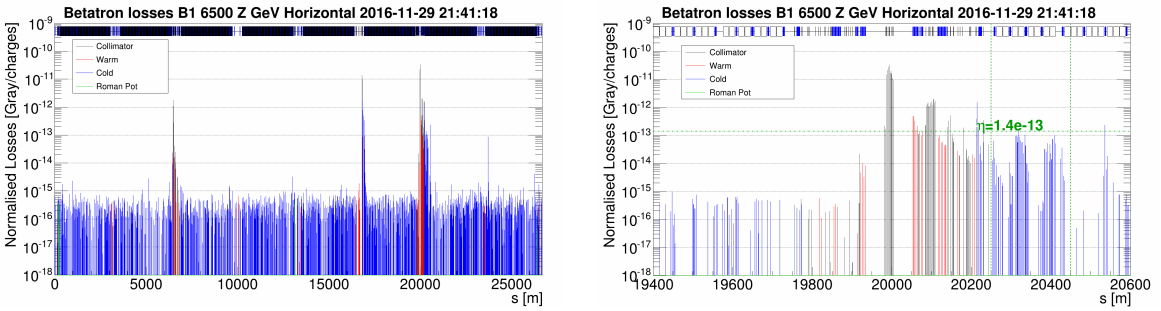

Figure 9: Horizontal crystal collimation loss maps. Settings 4 on Table 3. IR7 zoom is presented on the right.

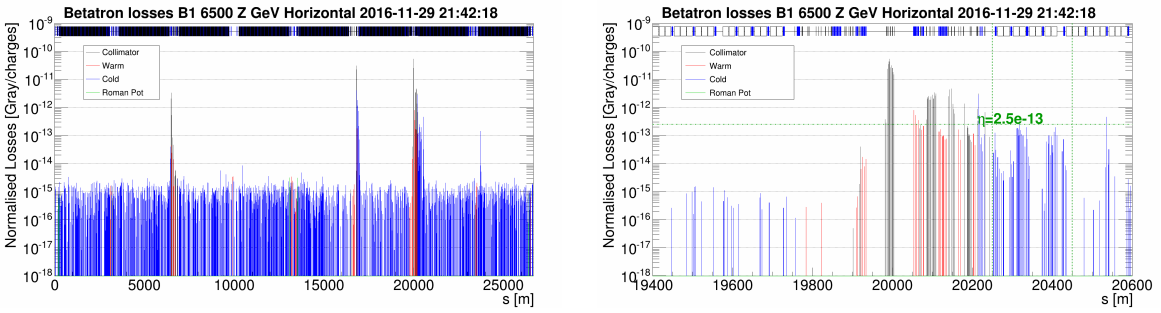

Figure 10: Horizontal crystal collimation loss maps. Settings 5 on Table 3. IR7 zoom is presented on the right.

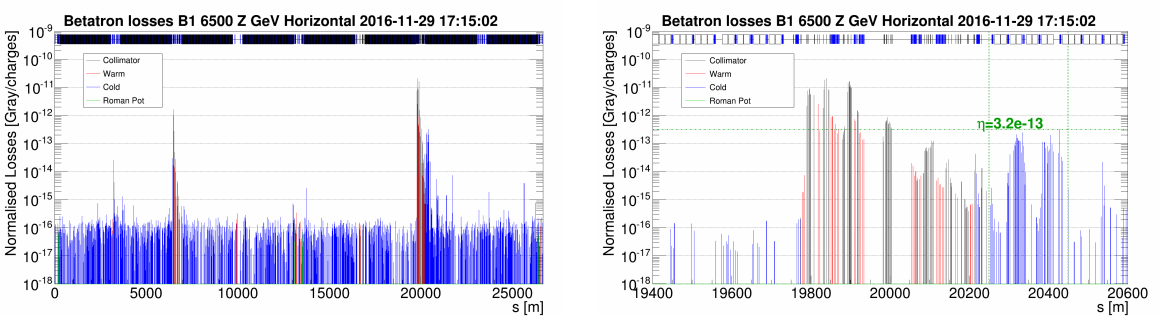

Figure 11: Vertical standard loss maps. IR7 zoom is presented on the right.

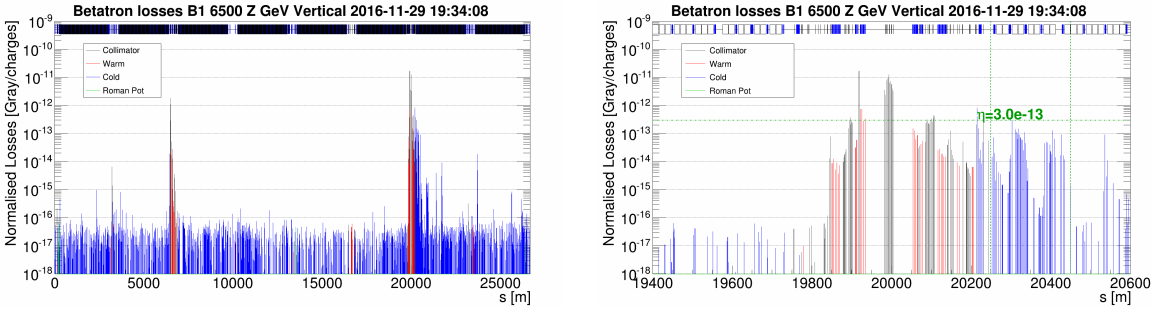

Figure 12: Vertical crystal collimation loss maps. Settings 1 on Table 3. IR7 zoom is presented on the right.

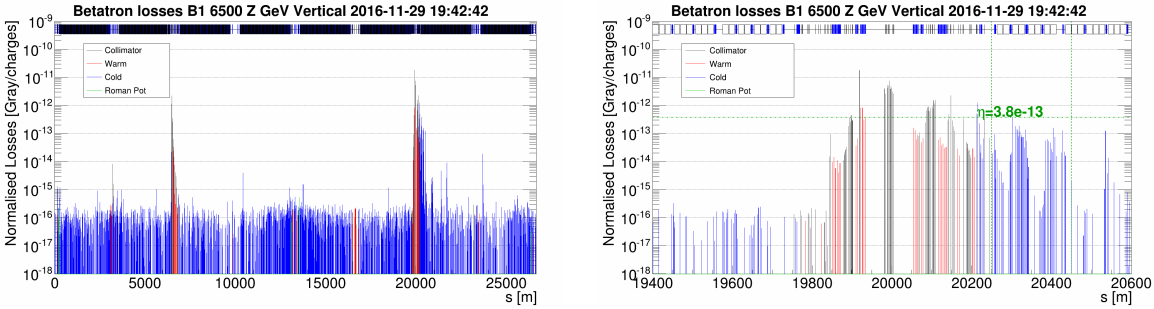

Figure 13: Vertical crystal collimation loss maps. Settings 2 on Table 3. IR7 zoom is presented on the right.

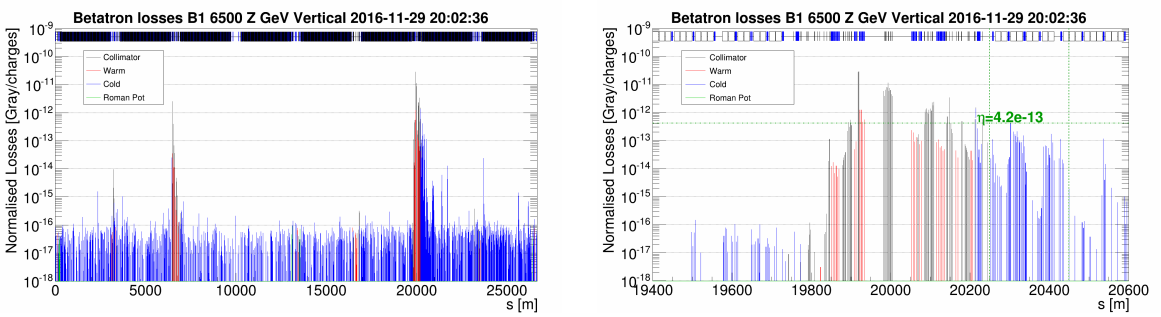

Figure 14: Vertical crystal collimation loss maps, crystal in amorphous orientation. Settings 3 on Table 3. IR7 zoom is presented on the right.

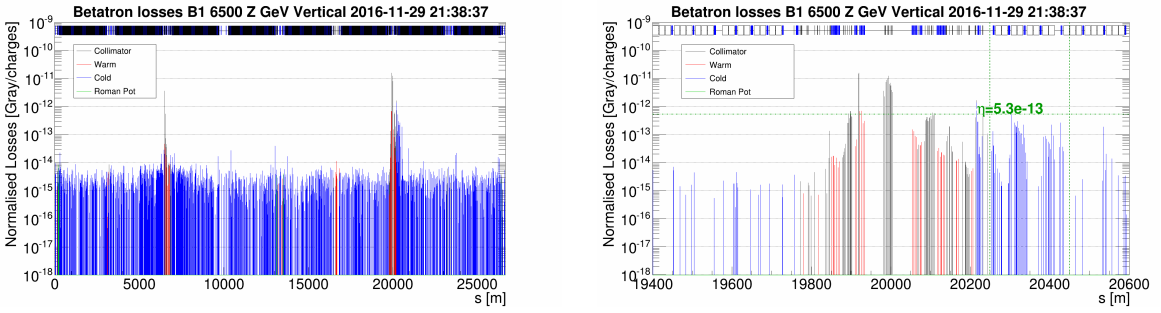

Figure 15: Vertical crystal collimation loss maps, crystal in amorphous orientation. Settings 4 on Table 3. IR7 zoom is presented on the right.

References

[1] R. Rossi et al., *Crystal Collimation with protons at injection energy*, MD Note, CERN-ACC-NOTE-2016-0035, 2016

[2] R. Rossi et al., *Crystal Collimation with protons at flat top energy*, MD Note, CERN-ACC-NOTE-2017-0021, 2017

[3] R. Rossi et al., *Crystal Collimation Cleaning Measurements with Proton Beams in LHC*, MD Note, CERN-ACC-Note-2018-0024-MD, 2018

[4] R. Rossi et al., *Crystal Collimation During the LHC Energy Ramp*, MD Note, CERN-ACC-Note-2018-0053-MD, 2018

[5] R. Rossi et al., *Crystal Collimation with Lead Ion Beams at Injection Energy in the LHC*, MD Note, CERN-ACC-Note-2018-0004-MD, 2018

[6] W. Scandale et al., *Comparative results on collimation of the SPS beam of protons and Pb ions with bent crystals*, Phys. Lett. B 703 547-551, 2011

[7] D. Mirarchi, *Crystal Collimation for LHC*, PhD Thesis, CERN-THESIS-2015-099, 2015

[8] W. Scandale et al., *Probability of inelastic nuclear interactions of high-energy protons in a bent crystal*, NIM B 268 2655-2659, 2010

[9] W. Scandale et al., *Volume reflection dependence of 400 GeV/c protons on the bent crystal curvature*, Phys. Rev. Lett. 101 234801, 2008